Available online at www.sciencedirect.com
SCIENCE DIRECT®
Journal of Pharmaceutical and Biomedical Analysis xxx (2005) xxx–xxx
JOURNAL OF PHARMACEUTICAL AND BIOMEDICAL ANALYSIS
www.elsevier.com/locate/jpba

A preliminary multi-stable-isotopic evaluation of three synthetic pathways of Topiramate

J.P. Jasper [a,*], L.E. Weaner [b], B.J. Duffy [b]

[a] *Molecular Isotope Technologies, LLC, 8 Old Oak Lane, Niantic, CT 06357-1815, USA*
[b] *Johnson & Johnson Pharmaceutical Research and Development, LLC, P.O. Box 776, Welsh and McKean Roads, Spring House, PA 19477-0776, USA*

Received 30 September 2004; received in revised form 6 March 2005; accepted 10 March 2005

Abstract

As a preliminary study of the utility of the natural stable-isotopic differentiation of batch samples produced by different synthetic pathways, multi-stable-isotopic analyses ($\delta^{13}C$, $\delta^{15}N$, $\delta^{18}O$, δD) of 53 samples of the antiepileptic drug, Topiramate, produced by three different synthetic pathways (designated "A," "B," "C") were performed. From the outset, we note that there are two fundamental variables that determine the stable-isotopic composition of materials—the stable-isotopic composition of the reagents and starting intermediates, and the isotope fractionation that occurs during manufacture of the product. In this study, the stable-isotopic composition of the raw materials was not controlled and we report here data obtained for a suite of samples that was produced by three synthetic pathways. Graphical examination of these data reveals marked data clustering by synthetic pathway, though in some cases with some overlapping values within standard errors. In general, the isotopic composition of Topiramate from the A and B pathways is distinct from the C pathway. The isotopic data from the A and B pathways typically abut each other, sometimes partially overlapping. The deuterium/hydrogen- (δD) and oxygen ($\delta^{18}O$) isotopic compositions are each significantly linearly related with the paired carbon ($\delta^{13}C$) isotopic composition indicating possible isotopic end-members for the raw materials of the present sample suite. Given that H and O typically derive from meteoric water, the linear correlations with $\delta^{13}C$ indicate that a mixture of carbon sources (viz., perhaps terrestrial C3 photosynthetic organic carbon and marine C3 organic carbon) were used in the production of the batches tested. If the H and O analyzed were derived from meteoric water, then an elementary comparison of the span of the δD ($\Delta\delta D = 54.6 \pm 2.1‰$) and of the $\delta^{18}O$ ($\Delta\delta^{18}O = 4.71 \pm 0.26‰$) values in the Topiramate samples to that of the global isotopic gradients indicates that the water retained in the samples spanned from as much as 11° of latitude (or, ~760 statute miles North-to-South). The present isotope results ($\delta^{13}C$, $\delta^{15}N$, $\delta^{18}O$, δD) form an initial database against which future samples can be compared to infer specific synthetic pathways. It is clear that to perform a rigorous test of the variables controlling the stable-isotopic composition of pharmaceutical materials that both the stable-isotopic composition of the starting materials and synthetic isotope fractionation must be controlled in future studies.

Keywords: Pharmaceutical materials; Active pharmaceutical ingredients; Synthetic pathways; Synthetic isotope fractionation; Topiramate; Stable isotopes; $\delta^{13}C$; $\delta^{15}N$; $\delta^{18}O$; δD

1. Introduction

Stable isotope-ratios have been used as tracers of source or "isotopic provenance" of natural materials since the 1950s when Isotope-Ratio Mass Spectrometers first became available [cf. 1,2]. In fact, 62 of the 112 elements are known to have at least 252 stable isotopes, yielding numerous possible isotopic-ratio tracers. Stable isotope measurements have been used to characterize different photosynthetic pathways that impart distinctive isotopic compositions to various plant organic materials [e.g., 3–5]. Such contemporary organic materials, ancient fossil fuel sources, and inorganic materials are used as raw materials in the production of active pharmaceutical ingredients (APIs, drug substances), excipients ("inactive components"), and drug products (finished dosage forms).

* Corresponding author. Tel.: +1 860 739 1926; fax: +1 860 739 3250.
E-mail address: jpjasper@molecularisotopes.com (J.P. Jasper).

0731-7085/$ – see front matter © 2005 Published by Elsevier B.V.
doi:10.1016/j.jpba.2005.03.011

The mechanisms that determine the isotopic compositions of plant materials are functions of different thermodynamic and kinetic parameters and are isotope dependent. For carbon, the isotopic composition of the atmospheric air and the isotopic fractionations caused by CO_2 transport and enzymatic fixation are key variables. Similarly, for nitrogen uptake, the isotopic composition depends on its speciation, transport, and fixation. Hydrogen and oxygen ratios are substantially affected by the isotopic composition of environmental water and fractionation that occurs during plant transpiration.

Determination of the light stable isotope-ratios, particularly, $^{13}C/^{12}C$, $^{15}N/^{14}N$, $^{18}O/^{16}O$, and D/H, have been previously used to trace the source of various natural products [e.g., 6–9]. When measured in drug products or in APIs, the stable-isotopic composition observed is the result of two variables: (i) the isotopic composition of the contributing raw materials ("thermodynamic fractionation") and (ii) the isotopic fractionation that often occurs during synthesis ("kinetic fractionation"; cf. [10]).

Pharmaceutical products can be characterized or "isotopically fingerprinted" by measuring and comparing their highly specific stable-isotopic ratios via isotope-ratio mass spectrometric analysis [11,12, and refs. therein]. As noted, the isotopic composition observed is dependent on both the isotopic composition of the reactants used and on the synthetic isotopic fractionation of the manufacturing process employed. A change in either of these variables produces a drug product having a different isotopic profile. Recent work has shown that when both the source of the starting materials and the manufacturing process are presumably held relatively constant during manufacture of the bulk drug substance, similar product isotopic-ratios are observed [13]. By measuring the isotopic ratios for suspect samples in various identity-fraud-related cases, including pharmaceutical counterfeiting, diversion (e.g., re-importation), theft, vicarious liability, and process patent infringement, it may be possible to obtain useful information about the process and origin of starting materials used.

When chemical reactions do not proceed to completion, or when multiple products are formed, light- and heavy isotopes are commonly distributed unevenly among reactants and products. Such isotopic inhomogeneities are referred to as fractionations. In principle, the isotopic compositions of chemical products can be predicted from the isotopic compositions of the starting materials together with knowledge of the fractionations. The latter can, however, be predicted quantitatively only when complete mass balances are available and when the kinetic and equilibrium isotope effects associated with all relevant chemical reactions are known accurately. Hayes [10] has discussed related calculations. Fortunately, isotopic analyses are inexpensive and precise, and allow isotopic compositions to be measured rather than predicted. Calculations do, however, provide a means of estimating ranges of variation. In future work, we will expand the scope of analyses so that the power of multiple stable-isotopic tracing can be adjudged in detail.

The isotopic composition of starting materials, intermediates, and final products can be directly measured if adequate samples are available. Determination of the specific isotopic fractionation for each reaction step requires precise isotopic measurements of the reactants and products [10]. This typically is determined by measurement of the stable-isotopic composition of the reagents used in a reaction, of the product(s) formed (e.g., mass balance and isotope mass balance [3]), and for a series of reactions (e.g., photosynthetic fractionation of CO_2 to specific organic compounds [14]). In practice, it is frequently difficult to retrieve samples of all of the starting materials needed to reconstruct a particular synthetic isotopic fractionation ratio. Recent observations, however, have indicated or shown that the stable-isotopic compositions of raw materials used in the synthesis of analgesic drug products gave characteristic and highly specific "isotopic fingerprints" for the individual batches tested [3,13,15]. For these samples, the dynamic ranges of the isotopic measurements were determined [13,15] and found to have a specificity of 1:469,000. That is, to a first approximation, there is only ~1 chance in 469,000 that the observed isotopic fingerprint would be found in a reproduction of the given product from raw materials with randomly distributed stable-isotopic compositions of the raw materials. The data suggest that if key variables are held relatively constant during the manufacture of bulk API, a clustering of the isotopic compositions is observed [e.g., 3,15].

To examine the potential of the technique for use in cases of counterfeiting and process patent infringement, the stable-isotopic composition of a suite of Topiramate API samples were examined via isotope-ratio mass spectrometry (IRMS) to determine whether this method can distinguish the isotopic provenance of batches produced by three different synthetic pathways. Four isotopic ratios ($\delta^{13}C$, $\delta^{15}N$, δD, $\delta^{18}O$) were examined and their results examined statistically and graphically.

2. Experimental

2.1. Isotopic analysis of Topiramate

Fifty-three samples of Topiramate ($C_{12}H_{21}NO_8S$; Fig. 1) were supplied by Johnson & Johnson Pharmaceutical Re-

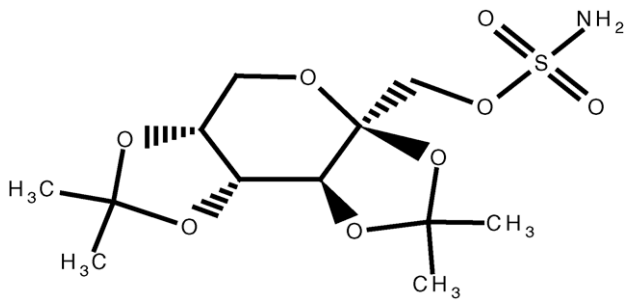

Fig. 1. Structure of the compound Topiramate ($C_{12}H_{21}NO_8S$).

Table 1
Stable-isotopic data for Topiramate samples

Sample ID	$^{13}C/^{12}C$	C:PldSE	$^{18}O/^{16}O$	O:PldSE	D/H	D:PldSE	C,O,D:*n*	$^{15}N/^{14}N$	N:PldSE	N:*n*
Synthesis A										
88 P 3519 Vial-1	−24.56	0.18	28.51	0.31	−135.2	1.8	1	−12.46	0.33	2
88 P 3519 Vial-2	−24.64	0.18	28.29	0.31	−129.0	1.8	1	−12.92	0.33	2
88 P 3519 Vial-3	−24.64	0.18	29.04	0.31	−134.7	1.8	1	−13.16	0.33	2
88 P 4189-D1	−25.05	0.12	28.78	0.23	−135.7	1.8	1	−14.13	0.22	4
88 P 4189-D3	−25.62	0.12	28.62	0.23	−137.0	1.8	1	−14.04	0.31	2
90 P 9355	−25.63	0.12	28.82	0.23	−133.4	1.8	1	−13.72	0.31	2
90 P 9356 rep-1	−25.69	0.07	28.38	0.13	−134.8	1.1	3	−19.50	0.31	2
90 P 9356 rep-2	−25.75	0.07	28.27	0.13	−134.3	1.1	3	−19.54	0.31	2
90 P 9356 rep-3	−25.46	0.07	28.39	0.13	−133.6	1.1	3	−19.38	0.31	2
Synthesis B										
10 403 092 Vial-1	−25.47	0.18	28.54	0.31	−134.1	1.8	1	−14.52	0.33	2
10 403 092 Vial-2	−25.63	0.18	29.00	0.31	−137.6	1.8	1	−14.77	0.33	2
10 403 092 Vial-3	−25.47	0.18	29.15	0.31	−135.0	1.8	1	−14.35	0.23	4
10 403 218	−24.51	0.12	28.60	0.23	−132.1	1.8	1	−12.20	0.31	2
10 403 554	−24.00	0.12	29.52	0.23	−132.0	1.8	1	−13.02	0.22	4
10 404 002	−25.88	0.12	28.05	0.23	−118.9	1.1	1	−12.75	0.22	4
10 404 114 rep-1	−25.74	0.07	27.82	0.13	−121.6	1.1	3	−13.35	0.25	3
10 404 114 rep-2	−25.95	0.07	27.70	0.13	−121.3	1.1	3	−12.86	0.25	3
10 404 114 rep-3	−25.78	0.07	28.36	0.13	−123.2	1.8	3	−12.54	0.43	1
10 404 233 Vial-1	−24.70	0.18	28.40	0.31	−128.3	1.8	1	−11.95	0.33	2
10 404 233 Vial-2	−24.12	0.18	28.81	0.31	−130.8	1.8	1	−12.00	0.33	2
10 404 233 Vial-3	−24.41	0.18	28.41	0.31	−126.1	1.8	1	−11.91	0.23	4
10 404 352	−24.44	0.12	28.57	0.23	−127.7	1.8	1	−12.27	0.31	2
10 404 471	−18.07	0.12	27.39	0.23	−84.6	1.8	1	−14.93	0.31	2
10 404 597	−18.24	0.12	27.35	0.23	−83.0	1.1	1	−14.13	0.31	2
10 404 716 rep-1	−23.11	0.07	29.63	0.13	−122.4	1.1	3	−13.45	0.22	4
10 404 716 rep-2	−23.12	0.07	30.14	0.13	−119.1	1.1	3	−13.07	0.31	2
10 404 716 rep-3	−23.09	0.07	29.70	0.13	−118.4	1.8	3	−13.71	0.31	2
10 404 835 Vial-1	−21.21	0.18	30.07	0.31	−95.5	1.8	1	−13.98	0.23	4
10 404 835 Vial-2	−21.56	0.18	29.76	0.31	−95.7	1.8	1	−13.99	0.23	4
10 404 835 Vial-3	−21.80	0.18	29.28	0.31	−96.5	1.8	1	−13.67	0.23	4
10 404 968	−24.25	0.12	30.45	0.23	−126.5	1.8	1	−13.05	0.22	4
10 405 087	−24.21	0.12	30.55	0.23	−128.1	1.1	1	−15.63	0.43	1
10 405 206 rep-1	−24.30	0.07	29.58	0.13	−128.7	1.1	3	−12.66	0.31	2
10 405 206 rep-2	−24.37	0.07	29.22	0.13	−129.1	1.1	3	−13.06	0.31	2
10 405 206 rep-3	−23.97	0.07	29.30	0.13	−130.0	1.8	3	−13.67	0.31	2
10 405 346 Vial-1	−24.34	0.18	29.47	0.31	−129.4	1.8	1	−13.64	0.33	2
10 405 346 Vial-2	−24.33	0.18	29.67	0.31	−128.2	1.8	1	−12.84	0.27	3
10 405 346 Vial-3	−24.41	0.18	29.21	0.31	−127.1	1.8	1	−13.26	0.33	2
Synthesis C										
9472–80 A Vial-1	−21.38	0.18	31.10	0.31	−110.3	1.8	3	−11.80	0.23	4
9472–80 A Vial-2	−21.29	0.18	30.51	0.31	−111.0	1.8	3	−11.92	0.33	2
9472–80 A Vial-3	−21.37	0.18	31.39	0.31	−110.3	1.8	3	−11.59	0.27	3
9482 -125	−19.02	0.12	30.72	0.23	−89.6	1.8	1	−16.69	0.31	2
9482–126	−18.84	0.12	30.66	0.23	−87.6	1.1	1	−17.66	0.31	2
9482–127 rep-1	−18.75	0.07	30.87	0.13	−87.2	1.1	3	−17.43	0.25	3
9482–127 rep-2	−18.70	0.07	30.58	0.13	−84.4	1.1	3	−17.57	0.25	3
9482–127 rep-3	−18.73	0.07	30.47	0.13	−90.3	1.8	3	−17.69	0.25	3
9482–153 Vial-1	−18.70	0.18	30.32	0.31	−84.2	1.8	1	−17.29	0.27	3
9482–153 Vial-2	−18.63	0.18	30.48	0.31	−89.3	1.8	1	−16.77	0.33	2
9482–153 Vial-3	−18.62	0.18	30.44	0.31	−89.1	1.8	1	−16.40	0.33	2
9482–178	−22.67	0.12	31.86	0.23	−115.8	1.1	3	−16.65	0.22	4
9482–185 rep-1	−22.66	0.07	31.70	0.13	−117.9	1.1	3	−17.05	0.22	4
9482–185 rep-2	−22.83	0.07	32.06	0.13	−114.4	1.1	3	−17.18	0.22	4
9482–185 rep-3	−22.68	0.07	31.95	0.13	−118.7	1.8	3	−17.47	0.31	2
Range	7.88		4.71		54.60			7.95		
Pooled S.D.	0.18		0.31		1.78			0.46		
Dynamic range	44.77		15.19		30.67			17.16		
Specificity									358137	
Sum of *n*							97			140
Total *n*										431

search and Development, LLC. All samples were analyzed for their stable-isotopic composition (δ^{13}C, δ^{15}N, δ^{18}O, δD) in varying degrees of replication (from $n = 1$ to 4; see Table 1). Individual samples of ~0.4 mg for δ^{13}C and δ^{15}N analysis were weighed and placed into tin boats that were crimped tightly around the analyte.

Carbon (δ^{13}C) isotopic analysis were performed with a Carlo Erba 1108 Elemental Analyzer interfaced via a Conflo II interface to a Finnigan MAT Delta Plus XL Isotope-Ratio Mass Spectrometer (EA/IRMS; [16]). The EA operated with an oxidation furnace temperature of 1020°C, reduction furnace temperature of 650°C, and a packed-column temperature of 60 °C.

2.2. Units of stable-isotopic measurement

Carbon isotopic results are typically expressed in δ-values (parts per thousand differences from international standards) defined as:

$$\delta 13C(‰) = ([(R_{smpl})/(R_{std})] - 1) \times 1000$$

where R_{smpl} is the $^{13}C/^{12}C$ ratio of the sample material and R_{std} is the $^{13}C/^{12}C$ ratio of an International Atomic Energy Authority Standard known as "VPDB", whose $^{13}C/^{12}C$ ratio has been defined as the official zero point of the carbon isotopic scale. Other stable isotope-ratios are analogously expressed. The observed isotopic ranges ($\Delta\delta$ in ‰) for all measured isotopes (C, N, O, H), the 1σ pooled standard deviations ($\pm$S.D. in ‰) and the resultant dynamic ranges (R_D, unitless) are reported here.

2.3. Carbon (δ^{13}C) and nitrogen (δ^{15}N) analyses

Single-to-quadruplicate measurements of carbon (δ^{13}C) and of nitrogen (δ^{15}N) were performed on each sample, as indicated in Table 1. Thus, averages of samples, as available, and their pooled standard errors [17] are reported there. In the case of a single measurement, the individual value is reported with the pooled standard errors based on a suite of sample replicates (discussed below). δ^{13}C values are reported relative to the International VPDB Standard δ^{15}N values are reported relative to the atmospheric air standard.

2.4. Hydrogen (δD) and oxygen (δ^{18}O) isotope analysis

Because D/H analyses of complex matrices have exchangeable D/H sites, all samples were equilibrated with water vapor by exposure to the laboratory atmosphere at room temperature for several days prior to analysis [18–21]. Following equilibration, individual samples of ~0.2 mg were weighed and placed into silver boats, which were then crimped tightly around the analyte. Single-to-triplicate hydrogen- (δD) and oxygen (δ^{18}O) stable-isotopic analyses of each sample were performed on a Finnigan Thermal Conversion/Elemental Analyzer (TCEA) interfaced to Finnigan Delta Plus XL Isotope-Ratio Mass Spectrometer (IRMS, thus a TCEA/IRMS). Analogous to a standard Elemental Analyzer/Isotope-Ratio Mass Spectrometer (EAMS; [16]), the TCEA functions with samples sequentially delivered into a furnace and the effluent gases analyzed by an online IRMS, but with pyrolysis (instead of oxidative combustion as in the EA/IRMS) performed at 1350°C. The TCEA thermally converts analytes to H_2 and CO rather than combustion into H_2O and CO_2 as in the EAMS. The analyte gases, H_2 and CO, are chromatographically separated on a packed column at 85°C. The mass spectrometer measures H_2 directly and ^{18}O in the form of CO. One-to-three measurements of hydrogen isotopic composition (δD) and of oxygen isotopic composition (δ^{18}O) were performed on each sample (Table 1). Averages of the measurements of each sample and their pooled standard errors are reported here. δD values are reported relative to the International VSMOW Standard. δ^{18}O values are reported relative to the International VSMOW Standard.

2.5. Statistical notes

While light isotope-ratio data are sometimes reported to three significant figures, the present data are reported to four significant figures because of their present high resolution and precisions (viz., pooled standard errors). To do otherwise would introduce an unnecessary granularity or coarseness into the estimation of precision and would mask the fine structure of the precision which is significant for following discussions (see Tables 1 and 2).

Fundamental statistical concepts of pooled standard deviation, dynamic range, and specificity were used to describe the stable-isotopic data presented here. Pooled standard deviations (PSD) of raw data were calculated to derive a representative standard deviation from the whole raw data set: small numbers of replicates (viz., $n = 1$–4) were pooled to derive an averaged standard deviation that is representative of the whole sample suite [17]. From those pooled standard deviations, pooled standard errors (PSE) were derived which scale the uncertainty of any given sample to the number of times it was analyzed; more specifically, PSE = PSD/(square root of $n - 1$), where n is the number of measurements performed on a given sample ([17]; Table 1). The dynamic range (R_D) is a dimensionless parameter defined as the observed range of the results divided by the pooled 1σ-standard deviations of the measurements (i.e., $R_D = \Delta\delta$/PSD; e.g., with $\Delta\delta = 10‰$ and with PSD = 0.1‰, $R_D = 10‰/0.1‰ = 100$), a quantitative parameter used to assess the granularity (or fineness) to which a measurement can be performed on a given suite of samples. With the first-order assumption that stable-isotopic values may be randomly distributed across their observed range, the probability of randomly selecting a given value would be 1/100 or 1% in the preceding example. Analogously, the probability of randomly selecting a sample with two or more specific isotopic values (each with its own $\pm 1\sigma - \delta$) would be the product

of the inverse of their composite dynamic ranges [e.g., $(PSD/\Delta\delta)_a \times (PSD/\Delta\delta)_b \times (PSD/\Delta\delta)_c = (1/100) \times (1/100) \times (1/100) = 1/106$]. This straightforward propagation of probabilities is termed "specificity." While in some natural products, certain isotopic values may be partially correlated, we adopt this easily reproducible, first-order estimate of statistical likelihood of occurrence in this early stage of stable-isotopic characterization of pharmaceutical composition.

Principal component analysis was performed on the data set shown in Table 1 using Matlab Version 6.1 (The Mathworks Inc., Natick, MA, USA) with the PLS Toolbox Version 3.0 (Manson, WA, USA). The replicate samples (replicates 1, 2, 3 or vials 1, 2, 3) were averaged so that they would not be disproportionately weighted. This reduced the 53 runs to 26 unique runs.

The data are displayed in three formats: bivariate graphs of principal component scores and bivariate- and trivariate isotope graphs. The principal-component format was chosen to determine clusters of samples that demonstrated similar isotopic characteristics due to given synthetic production pathways, though similar sources of raw materials cannot be eliminated in this preliminary study where that variable was not controlled. Bivariate graphs were produced to examine clustering of samples for two variables at a time; in this case, display of 1σ-standard errors permits the differentiation of batches from one another in these two isotopic dimensions. Trivariate graphs are shown to display the isotopic provenance simultaneously manifested by three different isotope-ratios in one plane.

3. Results

The isotopic ratios for 53 samples of Topiramate were measured with varying degrees of replication (from n = 1 to 4). A total of 431 isotopic measurements were performed on the samples, each for 4 isotopes, giving an average replication of ~2. In addition, two nitrogen standards were measured a total of 27 times to monitor instrument performance, yielding a total of 458 isotopic measurements that were performed for this study. A summary of the stable-isotopic data of Topiramate is given in Table 1 and the results are presented graphically in Fig. 3a–f.

3.1. Isotopic precision

The standard deviations of both the instrumental uncertainty and sampling-replicate (within-lot) uncertainty are given in Table 2. In all cases, the instrumental uncertainty is less than or equal to that of the sampling-replicate uncertainty. This observation is consistent with theory since instrumental uncertainty includes only the uncertainty generated by replication of ostensibly same samples. By contrast, the sampling-replicate uncertainty is expected to be of similar size or larger than the instrumental uncertainty since it is composed of the sum of both instrumental reproducibility and sampling (ir)reproducibility. The small observed differences between the sampling-replicate uncertainty and instrumental uncertainty in the present cases is quite small (markedly smaller than the instrumental uncertainty) and can be attributed to sampling uncertainty itself. From that, we conclude that the sampled lots were essentially isotopically homogeneous and that even singly measured samples are representative of their respective lots.

4. Discussion

4.1. Topiramate isotope data

4.1.1. Principal component analysis

The entire set of four-isotope-ratio data for 26 synthetic runs of Topiramate was subjected to principal component analysis. The data was normalized by dividing by the variance and mean centered. The 26 runs represented 4 runs for Synthetic Pathway A, 15 runs for Synthetic Pathway B, and 7 runs for Synthetic Pathway C. The scores plot of principal component 1 (PC1) versus PC2 showed the best discrimination between the three synthetic pathways.

The distribution of the principal component scores on a bivariate plot showed some segregation by synthetic pathway (Fig. 2). The Synthetic Pathway A data were clearly distinguished from the Synthetic Pathway C data. The data cluster for Synthetic Pathway B completely overlapped the data cluster for Synthetic Pathway A and partially overlapped the data cluster for Synthetic Pathway C. These general patterns are reproduced in the following stable-isotope bivariate plots.

4.1.2. Bivariate analysis

The six possible isotopic bivariate plots for the Topiramate are shown in Fig. 3a–f. All six graphs show a notable degree of sample clustering based on synthetic pathway. The data are clearly not randomly distributed. In general, the isotopic composition of Topiramate from the C pathway is non-overlapping with those of the A and B pathways. The A data

Table 2
Standard deviations of stable-isotopic measurements

Standard deviation	δ^{13}C (‰)	δ^{18}O (‰)	δD (‰)	δ^{15}N (‰)
Instrumental variability	0.12 (n = 18)	0.23 (n = 18)	1.8 (n = 18)	0.43 (n = 46)
Within-lot variability	0.18 (n = 21)	0.31 (n = 21)	1.8 (n = 21)	0.46 (n = 56)

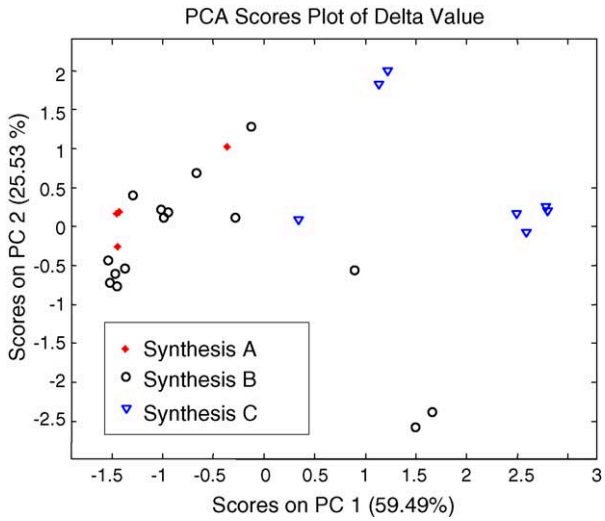

Fig. 2. Bivariate plot of principal component factors, as explained in text.

generally occur as two clusters, typically abutting clusters of B data. The B data generally form three-to-four clusters of variable sample density (or number). While the data may appear a bit scattered, they generally form three-to-four distinct clusters.

4.1.3. The relationship of $\delta^{13}C$ of Topiramate to δD and $\delta^{18}O$: photosynthetic pathways and meteoric water

Isotope bivariate plots of $\delta^{13}C$ versus δD and $\delta^{13}C$ versus $\delta^{18}O$ each show significant linear correlations (Fig. 3e–f). The plot of $\delta^{13}C$ versus δD is highly correlated with a correlation coefficient (r^2) of 0.890 ($n = 53$). While significant, the correlation coefficient of δ4/8/05 ^{13}C versus $\delta^{18}O$ is 0.458. In other words, the deuterium/hydrogen- (δD) and oxygen ($\delta^{18}O$) isotopic compositions of Topiramate are significantly linearly correlated with the paired carbon ($\delta^{13}C$) isotopic composition. Given that H and O typically derive from meteoric water, the linear correlations with $\delta^{13}C$ indicate that a mixture of carbon sources may have been used in the production of these Topiramate suites (discussed further below). If the H and O in the Topiramate samples that were analyzed derived from meteoric water, then an elementary comparison of the span of the δD ($\Delta\delta D = 54.6 \pm 2.1$‰) and $\delta^{18}O$ ($\Delta\delta^{18}O = 4.71 \pm 0.26$‰) values to the global isotopic gradients indicates that the water retained in the samples spanned from as much as 11° of latitude (or, ∼760 statute miles, North-to-South).

Linear correlations in stable-isotopic data are typically indicative of two end-member mixing systems (e.g., [20]). While an imperfect mixing system with some of the B data falling off the mixing line (Fig. 3e), the data are generally indicative of a two end-member mixing system. Simply judging from these data, one might ascertain that the $\delta^{13}C$ of ^{13}C-depleted end-member is ∼−26‰ versus VPDB and that the ^{13}C-enriched end-member is ∼−18‰ versus VPDB. The ^{13}C-depleted end-member (∼−26‰ versus VPDB) is typical of C3 photosynthetic terrigenous plants, while the ^{13}C-enriched end-member (∼−18‰ versus VPDB) is typical of C4 photosynthetic terrigenous plants and some algae [7,15]. Thinking it unlikely that algal components were used as raw materials for Topiramate, we can focus the discussion to infer that sources of C3 and C4 terrigenous organic matter were used in its synthesis. With that, we suggest that predominantly C3 organic carbon was used in the B pathway, while some B and C samples each appear to be a mixture of the two suggested end-member carbon sources since their values fall at various points along the putative mixing curve. By way of background, the δD and $\delta^{18}O$ of surface meteoric water is very highly correlated, spanning ∼350‰ in δD and ∼35‰ in $\delta^{18}O$ [21]. This excellent correlation exists in nature because of a process known as Rayleigh fractionation (or, isotopic distillation) of surface water as it is continuously evaporated and condensed in its general equator-to-poles' migration, thereby fractionally distilling the light- from heavy isotopes of water. We infer that hydrogen isotopes so-fractionated span from D-enriched, low-latitude environs (e.g., where $\delta D \sim -80$‰ in the Topiramate $\delta^{18}O$ record) where C4 plants predominate ($\delta^{13}C \sim -17$‰) to D-depleted, higher-latitude environs (e.g., where $\delta D \sim -140$‰) (see Fig. 3e).

The comparative scatter of the $\delta^{13}C$ versus $\delta^{18}O$ relationship (Fig. 3f) versus that of the $\delta^{13}C$ versus δD relationship (Fig. 3e) indicates that the suggested meteoric-water-line:photosynthetic pathway is not as well preserved in the Topiramate components in $\delta^{18}O$ versus δD. One might reasonably speculate that the ^{18}O in Topiramate is relatively more exchangeable than is the D. Laboratory D/^{18}O exchange studies could be performed to test such a mechanism.

4.1.4. Trivariate analysis

The data from all of the Topiramate samples examined in this study are combined in four trivariate-isotope plots (combinations of $\delta^{13}C$, $\delta^{15}N$, $\delta^{18}O$, δD; Fig. 4a–d). The plots have two general characters: the "DOC-" and "DNC" plots (Fig. 4a and b) have similar appearances, as do the "CON-" and "NOD" plots (Fig. 4c and d). While in the former plots ("DOC" and "DNC"; Fig. 4a and b), the Topiramate produced by synthetic pathways A and B are markedly overlapping at the visual level; in the latter plots ("CON" and "NOD"; Fig. 4c and d), they are markedly separated, making them more useful for product- and synthetic pathway differentiation. In plots "CON" and "NOD" (Fig. 4c and d), the three products and possibly their synthetic pathways appear markedly graphically different. Given that the standard errors are markedly non-overlapping (Table 1), statistical analyses of such widely separated points show that the samples are statistically different.

Condensing three dimensions into such trivariate or ternary isotope plots gives a very high information content for the whole data set and has a very fine 1σ grid spacing. In fact, there would be an average of ∼260,000 1σ grid points on Fig. 4a–d if we showed them all on each plot. In compensation, the sizes of error bars in such a plot are van-

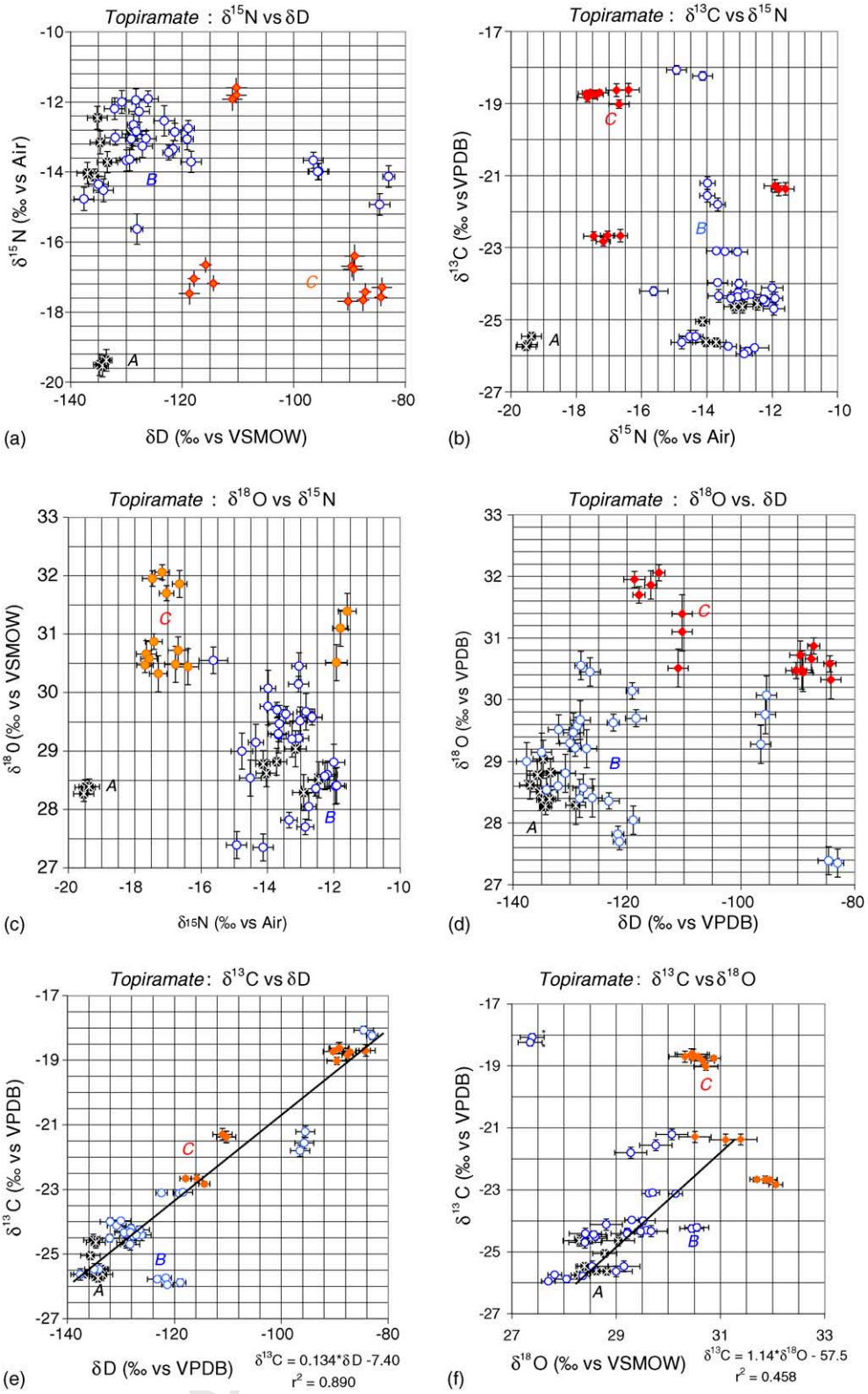

Fig. 3. Bivariate plots of stable-isotopic composition of the Topiramate sample suite mentioned in Section 2 (Fig. 3a–f): (a) δ^{15}N vs. δD; (b) δ^{18}O vs. δ^{15}N; (c) δ^{18}O vs. δ^{15}N; (d) δ^{18}O vs. δD; (e)δ^{13}C vs. δD and linear regression line; (f) δ^{13}C vs. δ^{18}O and linear regression line. Note that two outlying points (*) were not included in the regression.

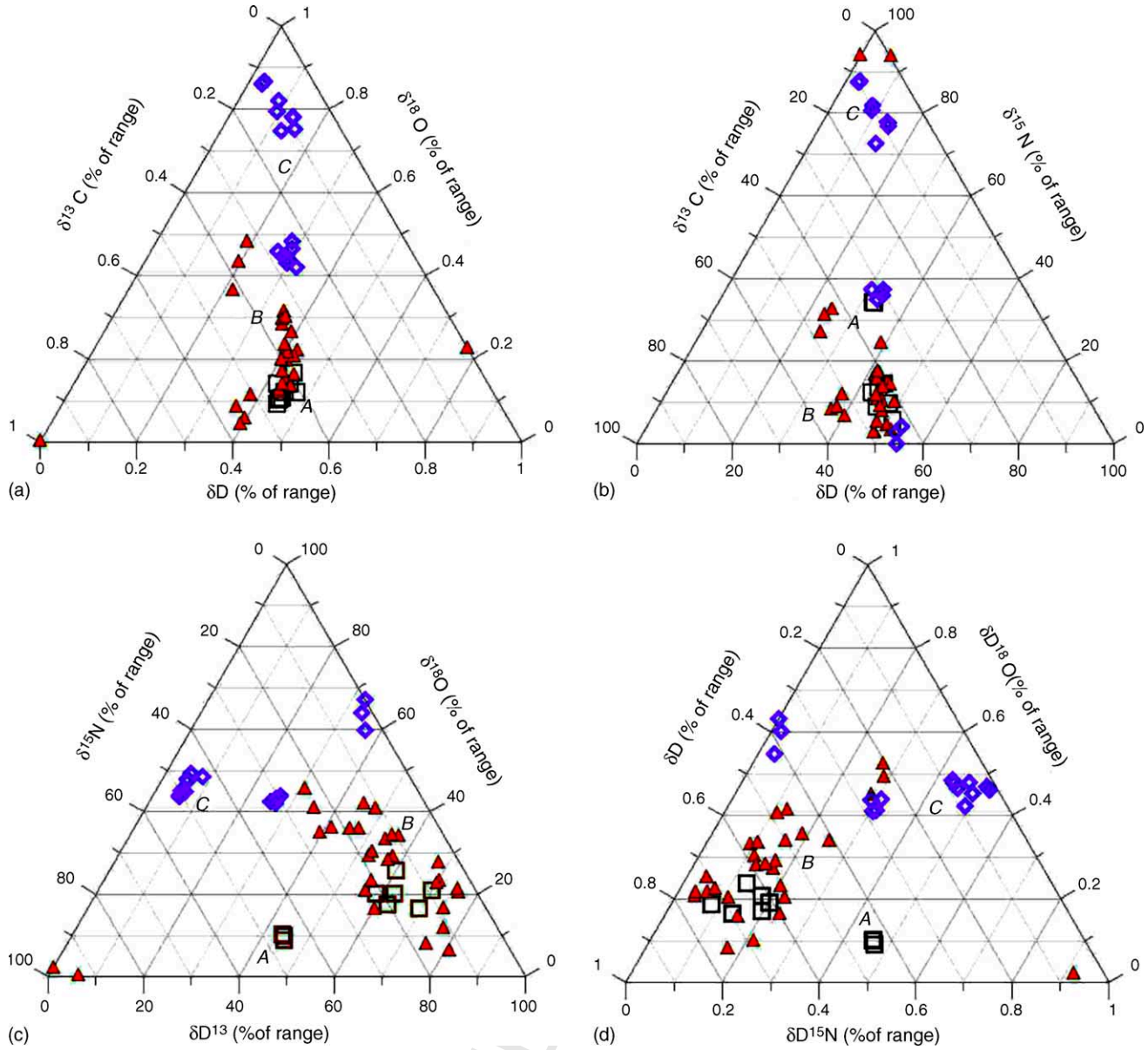

Fig. 4. Trivariate plots of stable-isotopic composition of the Topiramate sample suite mentioned in Section 2: (a) δD vs. δ^{18}O vs. δ^{13}C; (b) δD vs. δ^{15}N vs. δ^{18}O; (c) δ^{13}C vs. δ^{18}O vs. δ^{15}N; (d) δ^{15}N vs. δ^{18}O vs. δD.

ishingly small—on average, only ∼1% in each of the three dimensions—much smaller than the graph symbols themselves. Similar plotting of the isotopic compositions of other drug components in other studies has recently been found to be a useful means to present the "clustering" of the pharmaceutical stable isotopes in single plots, despite the loss of resolution of the uncertainty associated with each measurement.

4.2. Specificity of isotopic profiling of Topiramate

As noted, specificity is a numerical estimate of the relative uniqueness of a given material that can be used quantify the likelihood that another product with the same isotopic profile could be randomly produced from similarly variable raw materials and synthetic process. The dynamic ranges of δ^{13}C, δ^{15}N, δ^{18}O, and δD for the present suite of samples are given at the bottom of Table 1. The specificity of this Topiramate sample suite is ∼1:358,000. That is, the random possibility that a specific four-isotope "fingerprint" could be randomly reproduced from the same range of starting materials using the same synthetic pathways would be only ∼1 in 358,000.

For comparison, isotopic data for and calculations of specificity shown in Table 3 give a quantitative perspective on the scale of specificity achieved in the present study as compared to other plausible isotopic ranges. Viewed in an aggregate sense for purposes of discussion, these isotopic data for calculations of specificity show the many orders of magnitude

Table 3
Multi-isotope specificity for product authenticity

Isotope	Typical[a] $\Delta\delta$	Maximum[b] $\Delta\delta$	Maximum $\Delta\delta$ of APIs[c]
$\delta^{13}C$	15 (0.1)	140 (0.01)	7.88 (0.18)
δD	80 (1.0)	624 (0.2)	54.6 (1.8)
$\delta^{15}N$	10 (0.1)	200 (0.02)	7.95 (0.46)
$\delta^{18}O$	20 (0.1)	160 (0.02)	4.71 (0.31)
Specificity[d]	2.4×10^8	3.5×10^{15}	349×10^3
log (specificity)	9.8	15	5.5

[a] Typical $\Delta\delta$ are commonly occurring natural isotopic ranges [1,2] analyzed by an EAMS.
[b] Maximum $\Delta\delta$ values are maximum observed natural isotopic ranges [22] analyzed by dual-inlet mass spectrometers.
[c] Maximum $\Delta\delta$ of APIs represents a hypothetical combined API based on the samples reported in this study analyzed by an EAMS.
[d] Specificities are calculated as the product of the relevant dynamic ranges.

(viz., 5.5) are spanned for four sets of isotopic results presented. The specificity of typically occurring organic matter composed of C, N, H, and O is estimated at 2.4×10^8 [based on typical geochemical isotopic data (e.g., [2])]. An extreme high specificity of 3.5×10^{15} can be achieved by analysis of isotopically exotic, naturally occurring organic matter. The composite suite of the Topiramate yields a specificity of 358×10^3. Such specificity significantly limits the possibility of random—or even intentional attempts at—reproduction of a given Topiramate isotopic profile.

4.3. Tracing Topiramate synthetic pathways

The generation of the present isotope-ratio database provides an initial basis on which to compare other Topiramate samples and may be useful in determining the synthetic pathway used for a sample from an unknown source. However, as stated from the outset, isotopic provenance is a function of both equilibrium (viz., raw material) and kinetic (viz., synthetic pathway) fractionation. So, despite large potential differences in the isotopic compositions of starting materials, the synthetic fractionation of any given pathway could remain the same. On the other hand, if the isotopic compositions of starting materials were episodically varied in a series of batch production, then isotopic composition of the raw material could override the effect of synthetic isotope fractionation. This of course is not likely a problem for manufacturing processes that employ very similar raw materials and the same synthetic pathway from production batch to batch, which would yield characteristic relationships of isotopic provenance. For these samples the isotopic ratios can be used to identify a manufacturer's product in counterfeiting or product liability cases.

5. Conclusions

Multi-stable-isotopic analyses of a suite of Topiramate samples showed a high degree of isotopic provenance for four common stable isotopes: carbon ($\delta^{13}C$), nitrogen ($\delta^{15}N$), oxygen ($\delta^{18}O$), and hydrogen (δD). Plotting all six possible bivariate isotope graphs revealed the isotopic provenance of the three synthetic pathways of interest: A, B, and C. The isotopic profiles produced by pathway C are distinct from those observed for lots manufactured using pathways A and B. While the isotopic profiles of pathways A and B abut each other in some regions, they are significantly non-overlapping. The effects of Rayleigh Fractionation of meteoric waters and different photosynthetic pathways (C3, C4) may manifest themselves as linear correlations between $\delta^{13}C$ and δD and between $\delta^{13}C$ and $\delta^{18}O$. The $\delta^{13}C$ versus δD indicates that the carbon sources may be derived from a mixture of C3- and C4 photosynthetic pathways, with C3 plants more typical of higher latitudes and C4 plants more typical of lower latitudes. The present isotopic database forms a useful, initial basis for differentiating the provenance of other Topiramate samples. Further research, in which the measurement of the isotopic compositions of both the starting materials and final products, which will allow determination of synthetic isotope fractionations of reactions, is already underway. In theory, such research should result in well-defined clusters for products synthesized by specific synthetic pathways.

Acknowledgements

The authors thank Isotech Laboratories Inc. (Champaign, IL, USA) for production of the stable-isotopic data and Christopher D. Ellison, Mazen L. Hamad, and Robbe C. Lyon of the Division of Product Quality Research, Center for Drug Evaluation and Research, FDA for the principal component analysis and interpretation presented here. The concepts of quantitative, multi-isotopic characterization of batch-mode produced products ("isotope product authenticity") and of "natural labeling" are subject to pending patents in the G8 Countries and Australia held by Molecular Isotope Technologies, LLC.

References

[1] R.E. Criss, Principles of Stable Isotope Distribution, Oxford University Press, Oxford, UK, 1999, p. 254.
[2] J. Hoefs, Stable Isotope Geochemistry, Springer, New York, USA, 1997.
[3] J.P. Jasper, Pharm. Tech. 23 (1999) 106–114.
[4] J.R. Ehrlinger, J.F. Casale, M.J. Lott, V.L. Ford, Nature 408 (2000) 311–312.
[5] K.-U. Hinrichs, G. Eglinton, M.H. Engel, R.E. Summons, Geochem. Geophys. Geosys. 2 (2001), paper #2001GC000142 (forum).
[6] H. Craig, Geochim. Comsochim. Acta 3 (1953) 53–92.
[7] B.N. Smith, S. Epstein, Plant Physiol. 47 (1971) 380–384.
[8] R. Amundson, A.T. Austin, E.A.G. Schuur, V. Matzek, C. Kendall, A. Uebersax, D. Brenner, W.D. Baisden, Glob. Biogeochem. Cycl. 17 (2003) 1031, doi: 1029/2002GB001903.
[9] A. Longinelli, E. Selmo, J. Hydrol. 270 (2003) 75–88.
[10] J.M. Hayes, An Introduction to Isotopic Calculations, 2004, http://www.nosams.whoi.edu/docs/IsoCalcs.pdf.

[11] J.P. Jasper, Tablets Capsules 2(3) 37–42.
[12] J.P. Jasper, B.J. Westenberger, J.A. Spencer, L.F. Buhse, M. Nasr, J. Pharm. Biomed. Anal. 35 (2004) 21–30.
[13] J.P. Jasper, F. Fourel, A. Eaton, J. Morrison, A. Phillips, Pharm. Tech. 28 (2004) 60–67.
[14] J.P. Jasper, J.M. Hayes, Nature 347 (1990) 462–464.
[15] J.P. Jasper, F. Fourel, A. Eaton, J. Morrison, A. Phillips, Abstr. Am. Soc. Mass Spectrom., American Association of Mass Spectrometry, Chicago, IL, 2001.
[16] K. Habfast, in: I.T. Platzner (Ed.), Modern Isotope Ratio Mass Spectrometry, Wiley, New York, 1997, pp. 11–82.
[17] J.P. Jasper, Rap. Comm. Mass Spectrom. 15 (17) (2001) 1554–1557.
[18] A. Schimmelman, M.D. Lewan, R.P. Wintsch, 63(1999) 3751–3766.
[19] L.I. Wassenaar, K.A. Hobson, Environ. Sci. Technol. 34 (2000) 2354–2360.
[20] J.P. Jasper, R.B. Gagosian, Nature 342 (1989) 60–62.
[21] H. Craig, Science 133 (1961) 1702–1703.
[22] T.B. Coplen, J.A. Hopple, J.K. Bohlke, H.S. Peiser, S.E. Rieder, H.R. Krouse, K.J.R. Rosman, T. Ding, R.D. Vocke, K.M. Revesz, A.Lamberty, P.Taylor, P. De. Bievre, Compilation of Minimum and Maximum Isotope Ratios of Selected Elements in Naturally Occurring Terrestrial Materials and Reagents, US Department of the Interior, US Geological Survey, Water-Resources Investigations Report 01-4222, 98 pp.